

Implementation of 3 T Lactate-Edited 3D ^1H MR Spectroscopic Imaging with Flyback Echo-Planar Readout for Gliomas Patients

ILWOO PARK,^{1,2} ALBERT P. CHEN,³ MATTHEW L. ZIERHUT,² ESIN OZTURK-ISIK,² DANIEL B. VIGNERON,^{1,4}
and SARAH J. NELSON^{1,2}

¹UCSF/UCB Joint Graduate Group in Bioengineering, San Francisco, CA, USA; ²Surbeck Laboratory of Advanced Imaging, Department of Radiology and Biomedical Imaging, University of California San Francisco, 1700 4th Street, Room BH-303, San Francisco, CA 94158, USA; ³GE Healthcare, 11 Brunel Court, Suite 5116, Toronto, ON M5V3Y3, Canada; and ⁴Surbeck Laboratory of Advanced Imaging, Department of Radiology and Biomedical Imaging, University of California San Francisco, 1700 4th Street, Room BH-102F, San Francisco, CA 94158, USA

(Received 23 March 2010; accepted 12 July 2010; published online 23 July 2010)

Associate Editor Jeffrey L. Duerk oversaw the review of this article.

Abstract—The purpose of this study was to implement a new lactate-edited 3D ^1H magnetic resonance spectroscopic imaging (MRSI) sequence at 3 T and demonstrate the feasibility of using this sequence for measuring lactate in patients with gliomas. A 3D PRESS MRSI sequence incorporating shortened, high bandwidth 180° pulses, new dual BASING lactate-editing pulses, high bandwidth very selective suppression (VSS) pulses and a flyback echo-planar readout was implemented at 3 T. Over-prescription factor of PRESS voxels was optimized using phantom to minimize chemical shift artifacts. The lactate-edited flyback sequence was compared with lactate-edited MRSI using conventional elliptical k -space sampling in a phantom and volunteers, and then applied to patients with gliomas. The results demonstrated the feasibility of detecting lactate within a short scan time of 9.5 min in both phantoms and patients. Over-prescription of voxels gave less chemical shift artifacts allowing detection of lactate on the majority of the selected volume. The normalized SNR of brain metabolites using the flyback encoding were comparable to the SNR of brain metabolites using conventional phase encoding MRSI. The specialized lactate-edited 3D MRSI sequence was able to detect lactate in brain tumor patients at 3 T. The implementation of this technique means that brain lactate can be evaluated in a routine clinical setting to study its potential as a marker for prognosis and response to therapy.

Keywords—3D magnetic resonance spectroscopic imaging, *In vivo* lactate detection, Brain tumor, Glioblastoma multiforme.

INTRODUCTION

Lactate is a metabolic marker that is observed in many brain pathologies.^{8,11} Neoplastic processes that are present in tumors have low oxygen supply and depend on non-oxidative glycolysis for energy production.³¹ This means that lactate can be considered as an indicator of anaerobic glycolysis and reduced cellular oxygenation, which is of interest for evaluating response to radiation or other therapies. The potential for identifying regions of metabolic stress and ischemic area in brain means that *in vivo* measurements of lactate are of interest in patients with a number of different brain pathologies. Previous studies performed at 1.5 Tesla (1.5 T) have shown that the presence of lactate and lipid peaks in ^1H magnetic resonance spectroscopic imaging (MRSI) data is associated with a diagnosis of high-grade tumor.^{15,27} Elevated signals from lactate and lipid were associated with short survival in patients with glioblastoma multiforme (GBM) who were evaluated either prior to surgery or radiation treatment at 1.5 T.^{2,26} In these cases, increased lactate was interpreted as an indication of increased tumor metabolism and growth.^{1,24} The detection of lactate is thus of interest for evaluating prognosis and response to therapy in brain tumor patients.

^1H magnetic resonance spectroscopy (MRS) of lactate demonstrates two resonances: a doublet at 1.3 ppm from methyl protons (CH_3) and a quartet at 4.1 ppm from methine protons (CH). The methyl protons and the methine protons are weakly coupled to each other with a J-coupling constant of 6.93 Hz. For proton *in vivo* spectroscopy, the methyl doublet has been the target for lactate detection because the

Address correspondence to Ilwoo Park, Surbeck Laboratory of Advanced Imaging, Department of Radiology and Biomedical Imaging, University of California San Francisco, 1700 4th Street, Room BH-303, San Francisco, CA 94158, USA. Electronic mail: ipark@radiology.ucsf.edu

methine peaks are close to the water resonance and are not usually visible because of their relatively low signal intensity. Despite this advantage, the methyl doublet can be difficult to quantify because of lipid peaks, which overlap in the range of 0.9–1.3 ppm. In order to overcome this problem, a number of techniques have been developed to measure and separate the lactate doublet from lipid resonances.^{6,7,29}

One such technique is based on spectral editing using dual band selective inversion with gradient dephasing (BASING) pulses.²⁹ This technique allows for simultaneous detection of lactate at 1.3 ppm as well as uncoupled metabolites such as choline (Cho), creatine (Cr), *N*-acetyl-aspartate (NAA), and lipid. Based on J-difference editing, this technique exploits the fact that the phase of the doublet depends on the carrier frequency of the BASING pulse acting on the quartet at 4.1 ppm, which is weakly coupled to the doublet. The BASING pulse, which is a frequency selective inversion pulse surrounded by bipolar crusher gradients on orthogonal axes, places the methine quartet within the BASING inversion band for the first cycle (edit-on), while the carrier frequency of the BASING pulse is shifted in the second cycle so that the quartet is removed from the inversion band (edit-off).²⁹ As a result, the doublet becomes in-phase in the first cycle and 180° out-of-phase in the second cycle relative to uncoupled spins for echo time TE = 144 ms. Summing the two data sets provides only uncoupled spins including Cho, Cr, NAA, and lipid, whereas subtracting them renders only lactate (Fig. 1c).

Lactate editing combined with point resolved spectroscopy (PRESS) localized 3D MRSI has been applied to glioma patients at 1.5 T for non-invasive detection of lactate and other brain metabolites.^{2,15,26} These studies demonstrated the detection of lactate as well as Cho, Cr, NAA and lipid, and suggested that *in vivo* measurement of lactate as well as other MR-derived parameters may help in diagnosis and proper therapy selection for glioma patients. Although the increased signal strength at higher field is expected to enhance the sensitivity of brain metabolites including lactate, the detection of brain lactate using ¹H MRS based on J-difference editing at 3 Tesla (3 T) scanner has not been reported. Several studies have reported their unsuccessful attempts at measuring lactate in brain tumor patients using single voxel PRESS-localized MRS at 3 T.^{12,14} The poor lactate detection that was observed at 3 T in these studies was due to chemical shift mis-registration artifact caused by the limited bandwidth of refocusing pulses used for the localization of spectroscopic data.

Several studies have investigated the signal cancellation of J-coupled resonance due to the chemical shift difference between J-coupled spin partners in PRESS

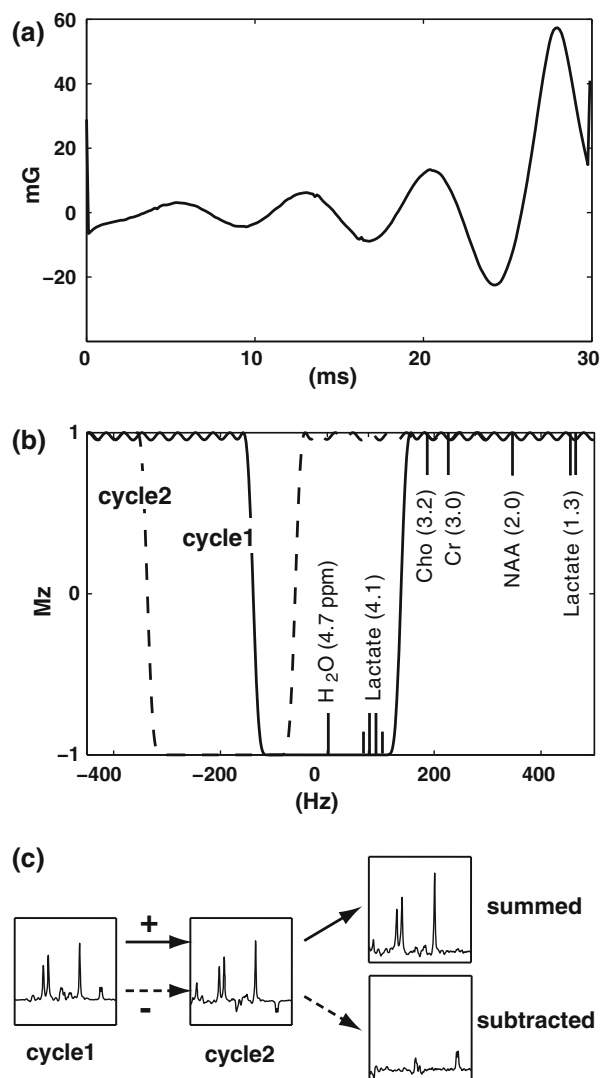


FIGURE 1. The new BASING pulse waveform designed for 3 T (a) and its inversion profile (b). Carrier frequency of the second cycle was shifted 198 Hz from the first cycle so that the lactate methine quartet was placed in either the passband or the stopband. As a result, lactate doublet is upright in one cycle and inverted in other cycle, so that summing the two data sets produces uncoupled resonances while subtracting them produces lactate resonance (c).

MRSI sequence in the context of lactate and GABA.^{9,10} This artifact is produced because spatially selective RF pulses cause a relative shift in the location of the selected volume for J-coupled resonances, thereby leading to net signal loss when the final signal is contributed from different regions. Kelley *et al.*¹⁰ demonstrated in phantoms that BASING pulses incorporated into non-editing PRESS sequence reduced the artifact for the detection of lactate methyl resonance in single voxel and MRSI data. For our editing scheme, this artifact may happen in the second cycle with BASING editing off, which is basically regular J-evolution. In the present study, we sought to

eliminate this artifact by using higher-bandwidth RF pulses since the spatial offset due to chemical shift difference is inversely proportional to RF bandwidth. In addition, we over-prescribed PRESS-localized volume and applied high bandwidth saturation pulses in order to further minimize this artifact.

The clinical use of lactate-edited MRSI based on J-difference editing has been limited by the requirement of two successive acquisitions per phase encoding step and the acquisition time which has typically been 20 min.¹⁵ Flyback echo-planar spectroscopic imaging has been used to allow the acquisition of MRSI data in a shorter scan time. Cunningham *et al.*³ demonstrated the feasibility and potential of MRSI data acquisition at 3 T with high spatial resolution and large coverage in a short scan time with flyback echo-planar readout gradient waveforms.

The purpose of this study was to implement a lactate-edited 3D PRESS ¹H MRSI sequence at 3 T with new high bandwidth 180° pulses, new BASING pulses and a flyback echo-planar readout gradient in order to allow a clinically suitable scan time of 10 min and demonstrate the feasibility of using this sequence for the detection of brain lactate as well as Cho, Cr, NAA, and lipid in patients. We addressed the effect of chemical shift artifact on lactate signal with different PRESS over-prescription (over-PRESS) factors and compared the metabolite SNR and its ratio of the lactate-edited MRSI data between a flyback echo-planar readout gradient method and conventional MRSI with elliptical *k*-space sampling. The method was then applied to patients with gliomas in order to determine whether it could detect lactate within lesions.

MATERIALS AND METHODS

Sequence Development and Implementation

Pulse sequence development and implementation were performed using the GE pulse sequence development environment (version 12x). The new 3 T dual BASING pulses were modified from the BASING pulses developed in our laboratory for application at 1.5 T²⁹ to accommodate the increased spectral range at

3 T. The new waveform, derived from the Shinnar-Le Roux algorithm,²³ had a duration of 30 ms and peak amplitude of 57 mG (Fig. 1a). The inversion and transition bandwidth of the waveform were 230 and 55 Hz, respectively (Fig. 1b). The sequence was modified so that the center of the BASING inversion band was placed at water (4.7 ppm) for the first cycle and shifted 198 Hz for the second cycle. As a result, the lactate methine peak (4.1 ppm) was placed within the BASING inversion band for the first cycle and removed from it in the subsequent cycle (Fig. 1b). The PRESS localization scheme incorporated shortened (6.5 ms) and higher-bandwidth (1.5 kHz) 180° refocusing pulses that were designed to minimize the effect of chemical shift mis-registration artifact at 3 T. The center frequency of 90° and 180° pulses was placed in the middle of lactate methyl and methine resonances at 2.64 ppm. New high bandwidth VSS pulses were custom-designed for 3 T with an 8.8 kHz bandwidth and 2 ms duration. The resulting 3D MRSI sequence consisted of a PRESS scheme incorporating new high bandwidth VSS pulses, higher-bandwidth 180° pulses, new 3 T dual BASING pulses positioned after the first and second 180° pulses and a flyback echo-planar readout gradient. Table 1 summarizes the various parameters for BASING, VSS, and PRESS pulses between the 1.5 T and the newly designed 3 T.^{16,29,30}

Estimation of Chemical Shift Artifacts with Over-PRESS Factors

The effect of chemical shift artifacts on the excitation profiles of lactate methyl and methine resonances was estimated by calculating the spatial offset of each resonance using the following equation²¹:

$$\Delta x = \frac{(w - w_0)}{BW_{RF}} \times X_{BOX}, \quad (1)$$

where Δx is the spatial offset of the excitation profile for a metabolite with resonance frequency w , from the carrier frequency, w_0 ; BW_{RF} is the bandwidth of the PRESS RF excitation pulse in the given direction (90° or 180°); and X_{BOX} is the width of the excited spectral region in that direction. Using Eq. (1), we estimated

TABLE 1. Comparison of BASING, VSS, and PRESS pulse parameters between the 1.5 T and the newly implemented 3 T sequence.

	BASING			VSS		PRESS	
	Peak amplitude (mG)	Inversion BW (Hz)	Transition BW (Hz)	BW (kHz)	Duration (ms)	90° pulse BW (Hz)	180° pulse BW (Hz)
1.5 T	30	100	55	6.5	3	2400	933
3 T	57	230	55	8.8	2	2400	1500

BW bandwidth.

the excitation profiles of lactate methyl and methine resonances for 1.2, 1.5, and 1.7 over-PRESS factors, defined as the ratio of the linear dimension of the excited volume to the prescribed volume. For simplicity, we considered only the x - y plane and assumed that the prescribed region is a 2D box with a size of 80×80 mm.

Spectroscopic Imaging

All spectroscopic imaging data were acquired using a 3 T Signa HDx (v12x) MR scanner (GE Healthcare, Milwaukee, WI) and an eight-channel phased array head coil. The spectroscopic imaging data were acquired with PRESS volume localization with an over-PRESS factor between 1.2 and 1.7. The over-PRESS factor was achieved by reducing the amplitude of the slice selection gradients. Chemical shift-selective saturation (CHESS) pulses were used for water suppression. VSS pulses of width 40 mm were placed on all sides of the prescribed volume to define the edges of the selected volume, and six additional graphic VSS bands were used in order to further improve the suppression of subcutaneous lipids for volunteer and patient scan. High-order shimming was performed prior to the MRSI data acquisition to optimize the magnetic field homogeneity. In order to estimate the sensitivity profile of each coil element, proton density weighted gradient-echo (GRE) images were acquired using the manufacture-provided parallel imaging (ASSET) calibration sequence (TR/TE = 150/20 ms).

Chemical Shift Artifacts with Different Over-PRESS Factors in Phantom

To study the effect of chemical shift artifacts for different over-PRESS factors and to determine an optimal over-PRESS factor for the new sequence, empirical data were obtained from a GE head MRS phantom containing 5 mM lactate as well as Cho (3 mM), Cr (10 mM), and NAA (12.5 mM).³⁰ 3D MRSI data were acquired with the excited volume of $80 \times 80 \times 40$ mm³ using over-PRESS factors of 1.2, 1.5, and 1.7 and VSS pulses around the prescribed volume (TR/TE = 1104/144 ms, FOV = $16 \times 16 \times 16$ cm, voxel size = $1 \times 1 \times 1$ cm, flyback echo-planar readout gradient in SI direction, 712 dwell points, 988 Hz bandwidth). In order to evaluate the variation in lactate signal across the excited volume for different over-PRESS factors, the mean value of lactate SNR was calculated from the right, left, middle, anterior, and posterior of the central two slices (Fig. 2). In addition, the peak height ratio of choline to NAA (Cho/NAA) was calculated and compared for three over-PRESS factors.

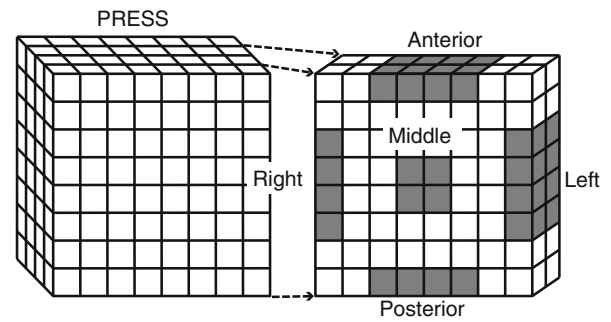


FIGURE 2. Lactate-edited 3D PRESS MRSI was applied to study the effect of chemical shift artifacts on lactate signal and other brain metabolites. The mean value of lactate SNR and choline to NAA ratio were calculated from the right, left, middle, anterior, and posterior voxels of the central two slices.

Comparison Between the Conventional Phase Encoding and Flyback Readout Gradient Methods

In order to compare signal quality between the conventional phase encoding and flyback readout gradient methods, a phantom and two volunteers were scanned using lactate-edited PRESS MRSI with both the conventional phase encoding (TR/TE = 1104/144 ms, FOV = $12 \times 12 \times 8$ cm, nominal voxel size = $1 \times 1 \times 1$ cm (1 cc), effective resolution = 2.5 cc, total acquisition time = 19 min, 1024 dwell points, and 2000 Hz bandwidth) and the flyback echo-planar readout gradient applied in SI (z) dimension (TR/TE = 1104/144 ms, FOV = $16 \times 16 \times 16$ cm, voxel size = $1 \times 1 \times 1$ cm (1 cc), total acquisition time = 9.5 min, 712 dwell points, and 988 Hz bandwidth). An over-PRESS factor of 1.5 was chosen for both methods. For the conventional MRSI method, an elliptical k -space sampling was applied so that the radius of the ellipsoid was chosen to reduce the acquisition time to approximately one-half of that of the full rectangular sampling.¹⁵ The number of phase encoding steps was reduced from 1152 ($12 \times 12 \times 8$) to 512 through zero filling the appropriate k -space points outside a normalized ellipsoidal radius of 1.2.³³ The SNR of Cho, Cr, NAA, and lactate were calculated from the middle four voxels of the central two slices for the phantom, and the SNR of Cho, Cr, and NAA in normal appearing white matter (NAWM) for the volunteers. The SNR of the flyback method was normalized to compensate for different scan times and effective spatial resolutions between the flyback and conventional MRSI methods by:

$$\text{nSNR}_{\text{flyback}} = \text{SNR}_{\text{flyback}} \cdot \frac{\sqrt{\text{TA}_{\text{conventional}}}}{\sqrt{\text{TA}_{\text{flyback}}}} \cdot \frac{\Delta V_{\text{conventional}}}{\Delta V_{\text{flyback}}}, \quad (2)$$

where $\text{nSNR}_{\text{flyback}}$ is the normalized SNR of flyback data, $\text{SNR}_{\text{flyback}}$ is the raw SNR of flyback data, TA is the total acquisition time, and ΔV is the effective spatial

resolution. The reduced elliptical k -space sampling in the conventional MRSI method resulted in an increase in the effective spatial resolution.^{17,18} A recent study has compared the effective spatial resolution between the elliptical k -space sampling in the conventional phase encoding method and the rectangular k -space sampling in the flyback method.³³ The authors used the spatial response function (SRF) generated by Fourier reconstruction in order to calculate the effective volume for each method and reported that the effective spatial resolutions for the conventional and flyback methods were 2.473 and 1.014 cm³, respectively. This resulted in an additional factor of 2.439 being required to correct for the difference between the effective spatial resolution of the conventional and flyback methods:

$$\Delta V_{\text{conventional}} = 2.439 \Delta V_{\text{flyback}} \quad (3)$$

This ratio was consistent with the previous finding, obtained by comparing the SNR of NAA in NAWM between the two methods.²² Considering both the effective spatial resolution and differences in scan time between the conventional and flyback methods, a factor of 3.4 was used to normalize the SNR of the flyback method.

$$n\text{SNR}_{\text{flyback}} = 3.4 \times \text{SNR}_{\text{flyback}} \quad (4)$$

Patient Data Acquisition

A total of 10 patients (eight male, two female, median age 55, range 41–64) with GBM were included in this study. Some patients had more than one examination and a total of 34 scans from these patients were examined to demonstrate the feasibility of using the new lactate-edited 3D MRSI sequence for the detection of lactate in brain tumor at 3 T. All patients were scanned using 3 T lactate-edited PRESS 3D MRSI sequence with the flyback echo-planar readout gradient applied in SI dimension using an over-PRESS factor of 1.5 (TR/TE = 1104/144 ms, FOV = 16 × 16 × 16 cm, voxel size = 1 × 1 × 1 cm, total acquisition time = 9.5 min, 712 dwell points, and 988 Hz bandwidth). The MRI protocol included an axial T2-weighted fluid attenuated inversion recovery (FLAIR) sequence⁴ with 3-mm slice thickness and axial pre- and post-gadolinium-DTPA T1-weighted spoiled gradient recalled (SPGR) images with 1.5-mm thickness. All patients provided informed consent as approved by the committee on human research at our institution.

Data Processing and Quantification

The method used for spectral quantification has been described previously.¹⁹ In brief, the 3D MRSI data with the conventional phase encoding were

reconstructed by processing each of the spectra from the eight-channel coil individually, apodizing with a 4 Hz Lorentzian filter in the time domain, zero filling to 1024 points, applying phase and frequency correction, and then removing residual water and baseline. The individual data were Fourier-transformed to produce a 3D spatial array of spectra and combined using in-house developed software that weights the data by their coil sensitivities from the low resolution proton density weighted images.^{16,25} The two cycles of data were then either summed or subtracted to produce a 3D array of summed or subtracted spectra.

The 3D MRSI data with the flyback echo-planar readout were reconstructed and combined in the same way as the data with the conventional phase encoding, but with the application of an additional linear phase correction in the SI dimension of spectral k -space to prevent spatial chemical shift artifacts.³ To reconstruct the data acquired with the flyback echo-planar readout gradient, only samples from the flat part (plateau) of the gradient waveforms were used.

The SNR of brain metabolites was calculated using the previously published method.²⁰ The region of 100 spectral points without metabolite signal was selected to estimate the standard deviation (SD) of the noise. Sub-regions with a size of 20, 40, and 80 points were made and located at the beginning of the selected region. The location of the sub-region was incremented by 1 point until it reached the end of the selected region, resulting in a total of 81, 61, and 21 divisions, respectively. For each sub-region, the SD was computed, the minimum SD was taken for each division, and the minimum SD of the divisions was used for the final SD of noise. The SNR of peak height over the SD of noise was calculated for Cho, Cr, NAA, and lactate.

In order to quantify lactate level in patients, median lactate SNR was estimated for each examination. Lactate peaks with SNR equal to or greater than 4 were only included in calculating the median lactate SNR. The estimation of lactate SNR was confined to the lactate appearing in contrast enhancing lesion (CEL) or T2 hyperintense region (T2h). The lactate found in resection cavity, necrotic region, or cerebrospinal fluid was excluded from the analysis.

RESULTS

Estimation of Chemical Shift Artifacts with Over-PRESS Factors

Figure 3 illustrates the effect of chemical shift misregistration artifact on the lactate excitation profiles for 1.2 and 1.5 over-PRESS factors. Using a 96 × 96 mm excited box with an 1.2 over-PRESS factor,

1500 and 2400 Hz bandwidth of the PRESS 180° (RL direction) and 90° pulses (AP direction), respectively, 170 Hz shift of lactate methyl resonance (1.3 ppm) from the carrier frequency (2.64 ppm), and the directionality information of the chemical shift artifact, Eq. (1) estimated the lactate methyl excitation profile (dashed line) to be shifted from the carrier frequency excitation profile (solid line) by 11 mm in RL direction and 6.8 mm in AP direction toward the top-left corner and the lactate methine excitation profile (dotted line) by 12 mm in RL direction and 7.5 mm in AP direction toward the bottom-right corner (Fig. 3a). As a result, it produces a region with a size of 73×82 mm (highlighted box) where both the lactate methyl and methine resonances are equally excited and a portion

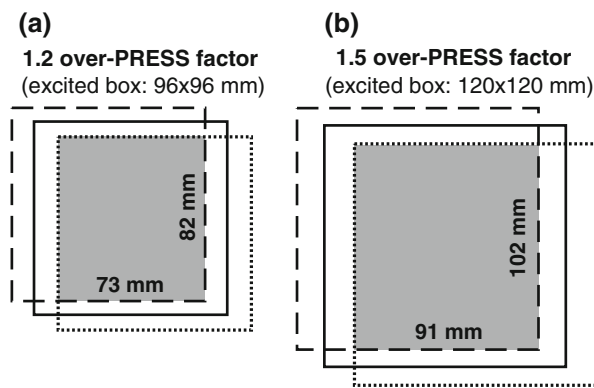


FIGURE 3. The illustration of chemical shift mis-registration artifact for 1.2 and 1.5 over-PRESS factors. The 1.2 over-PRESS factor produces shifted excitation profiles for lactate methyl (dashed line) and methine (dotted line) resonances from the excitation profile of carrier frequency (solid line), resulting in a 73×82 mm region with the simultaneous excitation of two lactate resonances (a). Similarly, the 1.5 over-PRESS factor produces a 91×102 mm region with the simultaneous excitation of two lactate resonances (b) and therefore smaller chemical shift artifacts compared to the 1.2 over-PRESS factor.

of the prescribed box in RL direction where only one of the lactate resonances is excited. Similarly, using an 120×120 mm and 136×136 mm excited box with the over-PRESS factors of 1.5 and 1.7, respectively, the 1.5 over-PRESS factor produces a 91×102 mm region (Fig. 3b) and the 1.7 over-PRESS factor a 104×116 mm region with the simultaneous excitation of two lactate resonances. Given the size of the prescribed box (80×80 mm), the chemical shift artifact is expected to be most pronounced with an 1.2 over-PRESS factor and more accentuated in RL direction compared to AP direction due to the lower bandwidth of 180° pulse (1.5 kHz) used for selection in RL direction compared to the bandwidth of 90° pulse (2.4 kHz) used for selection in AP direction. Our phantom data were consistent with this observation in that the chemical shift artifact manifested as the signal cancellation of lactate doublet was most apparent in the left column and improved with increases in the over-PRESS factor (Figs. 4 and 5).

The Effect of Chemical Shift Artifacts on Metabolite Signal in Phantom

As expected, the effect of chemical shift artifacts on lactate signal variation across the excited volume was reduced as the over-PRESS factor increased. Mean lactate SNR from the right, left, middle, anterior, and posterior voxels are plotted against the over-PRESS factors of 1.2, 1.5, and 1.7 in Fig. 4. The mean and SD of lactate SNR from the five locations are summarized in Table 2. The mean lactate SNRs were similar for different over-PRESS factors. In contrast, the SD of lactate SNR decreased with increases in the over-PRESS factor, indicating that the chemical shift mis-registration artifact lessened with increase in the over-PRESS factor. The lactate SNR from the left voxel showed the largest variation across the three

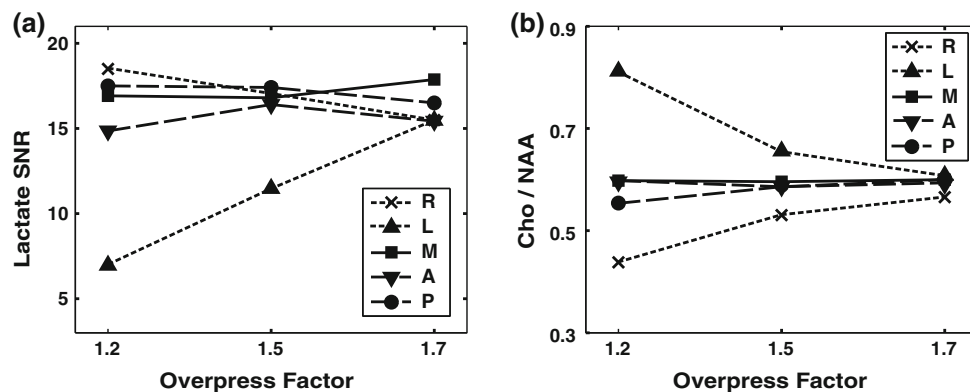


FIGURE 4. The effect of chemical shift artifacts on brain metabolite signal was evaluated using a phantom. Mean lactate SNR (a) and choline to NAA ratio (Cho/NAA) (b) were compared between the right (R), left (L), middle (M), anterior (A), and posterior (P) voxels of the excited volume. As the over-PRESS factor increased from 1.2 to 1.7, the chemical shift artifact lessened.

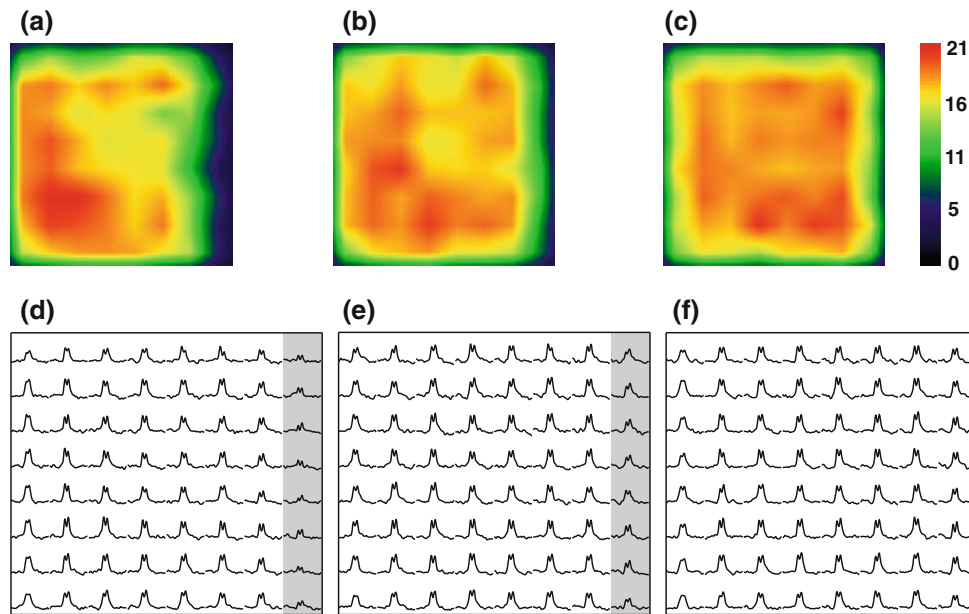


FIGURE 5. The distribution of lactate methyl doublet from MRSI data using phantom. The top images show the color maps of lactate SNR for the over-PRESS factors of 1.2 (a), 1.5 (b), and 1.7 (c). The corresponding spectra zoomed-in around lactate doublet are shown in the bottom for the over-PRESS factors of 1.2 (d), 1.5 (e), and 1.7 (f). The lactate doublet in the left column (highlight) had lower intensity compared to other regions of the PRESS volume for the over-PRESS factors of 1.2 and 1.5. The overall uniformity of lactate intensity increased with increases in the over-PRESS factor.

TABLE 2. Comparison between three over-PRESS factors.

	Over-PRESS factor		
	1.2	1.5	1.7
Lactate SNR	15 (4.7)	16 (2.5)	16 (1.1)
Cho/NAA	0.60 (0.14)	0.59 (0.04)	0.59 (0.02)

The mean and SD of lactate SNR and choline to NAA ratio (Cho/NAA) across the five regions of the excited volume for different over-PRESS factors. The numbers inside parenthesis indicate the SD.

over-PRESS factors and rapidly increased with increases in the over-PRESS factor. The differences between the lactate SNR from the left and right voxel were 12 and 6 for the over-PRESS factors of 1.2 and 1.5, respectively, and hardly noticeable for the over-PRESS factor of 1.7 (Fig. 4a). The Cho/NAA displayed a similar pattern. The Cho/NAA values from the different regions of the excited volume converged as the over-PRESS factor increased, whereas the mean Cho/NAA from the five regions were similar across the three over-PRESS factors (Table 2). Figure 5 shows the color-maps of lactate SNR and the corresponding lactate spectra for the three over-PRESS factors. The spectra were taken from the central slice of the PRESS 3D volume. The color maps were generated by spatially interpolating lactate SNR values to the resolution of anatomical images using a linear kernel. The map with an 1.2 over-PRESS factor showed a large

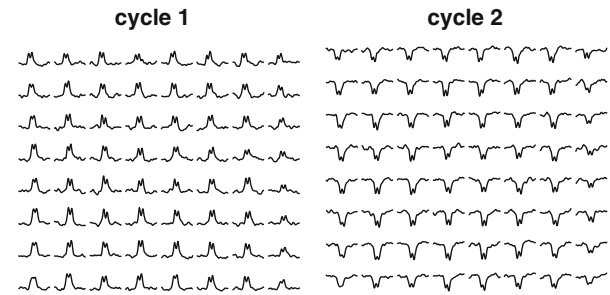


FIGURE 6. Lactate spectra from the first (edit-on) and second (edit-off) cycles acquired from phantom using the over-PRESS factor of 1.5. The use of higher-bandwidth 180° refocusing pulses in combination with over-prescription and high bandwidth VSS pulses minimized signal cancellation across the excited volume and provided relatively uniform lactate signal for both data sets.

signal drop-off in the left region of the spectra, which was alleviated with an 1.5 over-PRESS factor. The map with an 1.7 over-PRESS factor showed fairly uniform signal intensity across the entire region.

The artifact caused by the spatial interference of lactate methyl and methine spins appeared to be minimal. Figure 6 shows MRSI data sets zoomed-in around lactate doublet from the BASING edit-on (first cycle) and edit-off (second cycle) scans with an 1.5 over-PRESS factor. The lactate doublets from the first and second cycles were relatively uniform throughout the excited volume with a slight signal drop-off in the left column. The intensity and distribution of lactate

from the second cycle were similar to those from the first cycle, except that they are 180° out-of-phase to each other. It indicates that the use of higher-bandwidth 180° pulses in combination with over-PRESS and high bandwidth VSS pulses was able to minimize the chemical shift artifact.

Comparison Between the Conventional Phase Encoding and Flyback Readout Gradient Methods

Lactate-edited MRSI spectra acquired with a flyback readout gradient demonstrated excellent detection of uncoupled spins in the summed spectra and lactate in the subtracted spectra for phantoms and volunteers. The over-PRESS and use of high bandwidth VSS pulses provided minimal chemical shift mis-registration. Figure 7 shows an example of spectroscopic voxels from the lactate-edited MRSI with a flyback echo-planar readout gradient in a phantom (a, b) and a volunteer (c, d). In the subtracted spectra (b, d), the lactate doublet at 1.3 ppm was observed in the phantom data (b), but not in the healthy volunteer (d).

Cho, Cr, and NAA were summed (a, c) or removed (b, d) for both the phantom and volunteer. The median raw SNR of Cho, Cr, and NAA from the flyback method was 50, 60, and 84 for phantom and 10, 8, and 19 for volunteers, respectively. The median raw SNR of lactate from the flyback method was 18 for the phantom. The median normalized SNR values of brain metabolites and their ratios from the flyback method are compared to those from the conventional phase encoding method for phantom and volunteers in Table 3. The signal reduction for the flyback method compared to the conventional phase encoding ranged from 17 to 22% in the phantom and 19 to 25% in volunteers for Cho, Cr, NAA, and lactate (Table 3). An example of spectra from a volunteer comparing the two MRSI methods is shown in Fig. 8.

Patient Data from the Lactate-Edited 3D MRSI with a Flyback Gradient

Seven patients showed the presence of lactate peaks and lactate with a SNR greater than 4 was observed in

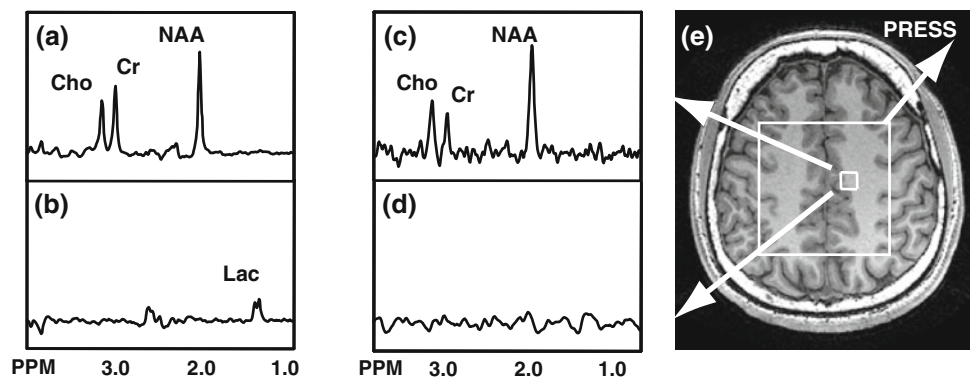


FIGURE 7. Lactate-edited spectra with a flyback gradient in a phantom (a, b) and a volunteer (c, d). Lactate is detected in the subtracted spectrum of phantom (b), and uncoupled resonances are produced in summed spectra in both phantom (a) and volunteer (c). T1-weighted image from the volunteer (e) shows the PRESS box and the voxel chosen for the spectra.

TABLE 3. The median SNR values and metabolite ratios of brain metabolites for raw flyback, normalized flyback, and conventional MRSI methods.

	Phantom ($n = 1$)			Volunteer (NAWM, $n = 2$)			Patients (NAWM, $n = 33$)	
	rFB	nFB	cMRSI	rFB	nFB	cMRSI	rFB	nFB
Cho	50	173	208	10	35	43	10	34
Cr	60	207	262	8	29	39	8	28
NAA	84	288	349	19	66	85	17	59
Lac	18	61	78				5 ^a	17 ^a
Cho/NAA	0.60		0.60	0.53		0.51	0.59	
Lac/NAA	0.21		0.22				0.30 ^a	

NAWM normal appearing white matter, rFB raw flyback, nFB normalized flyback, cMRSI conventional MRSI with elliptical k -space sampling, Cho/NAA choline to NAA ratio, Lac/NAA lactate to NAA ratio.

^aLactate in patients was measured from the contrast enhancing lesion or T2 hyperintense region and lactate in necrosis or resection cavity was excluded.

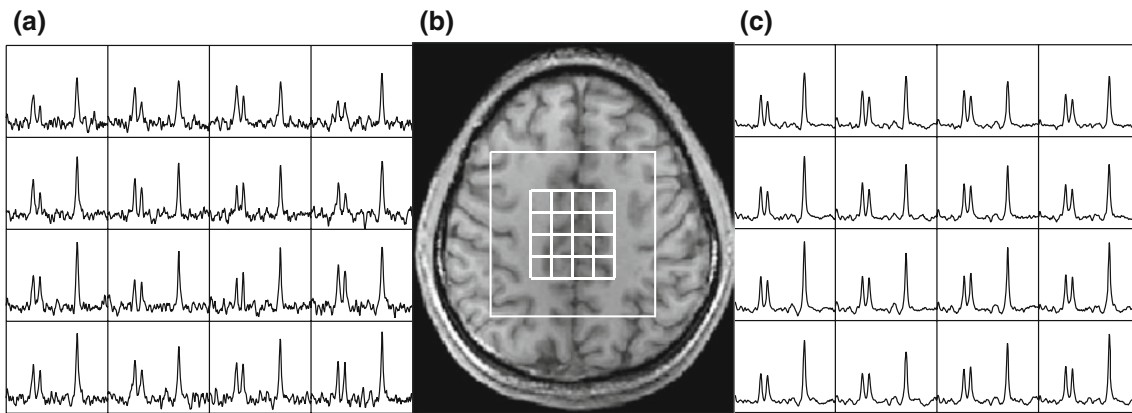


FIGURE 8. Comparison of MRSI data between the flyback-gradient method (a) and the conventional elliptical MRSI method (c) from a volunteer. T1-weighted SPGR (b) shows PRESS box and the spectral array.

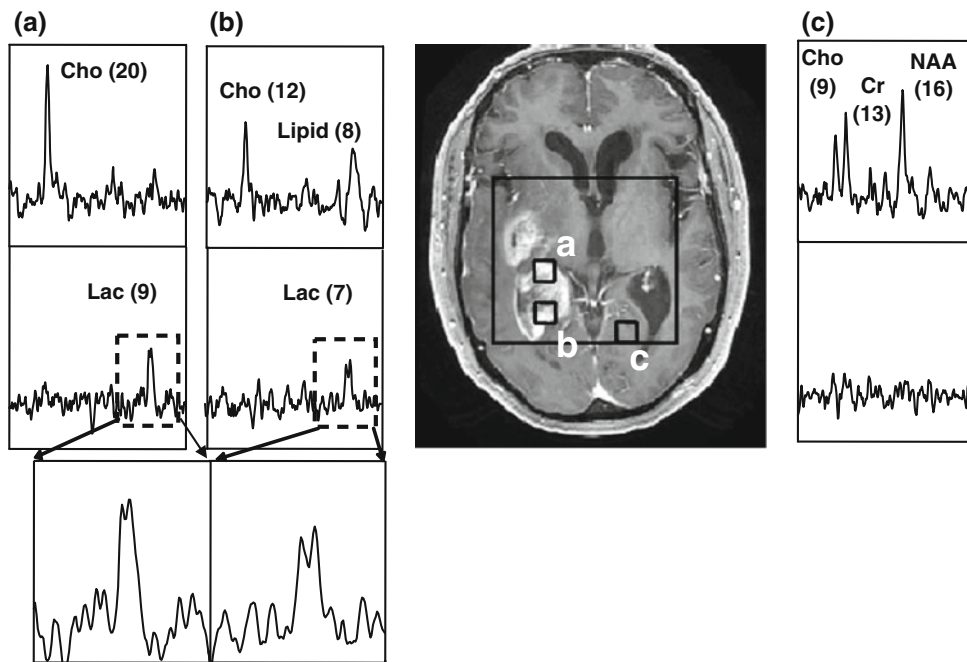


FIGURE 9. An example of lactate-edited spectra using the flyback-gradient method from a patient. The voxels in contrast enhancing lesions (a, b) contain high choline (Cho) as well as lipid in summed spectra (top) and lactate in subtracted spectra (bottom). The normal tissue from contra-lateral hemisphere (c) shows normal display of brain metabolite level (top in c) without lactate (bottom in c). The numbers indicate raw SNR values.

a total of 14 examinations. The median normalized SNR of lactate in those patients was 17. The SNR of Cho, Cr, and NAA in NAWM from all patients were similar to the values in NAWM from normal volunteers (not significantly different in a Mann–Whitney rank sum test with $p > 0.4$) (Table 3). The Cho/NAA in NAWM from the patients were similar to the values from healthy volunteers (not significantly different in a Mann–Whitney rank sum test with $p > 0.3$) and comparable to the values reported in several literatures.^{5,32} An example of data from a patient who had

lactate in the CEL is shown in Fig. 9. Voxel (a) and (b) were taken from the CEL in the T1-weighted post-contrast image, and voxel (c) was taken from the normal tissue in the contra-lateral hemisphere. The voxels in the top row are summed spectra, and the voxels in the bottom row are subtracted spectra. High Cho levels were observed in the summed spectrum of the voxel (a) and (b), which is characteristic of tumor, and the presence of lipid in the summed spectrum of the voxel (b) may indicate necrosis. Lactate appeared in the voxels with lesions (a, b). Lactate doublets were

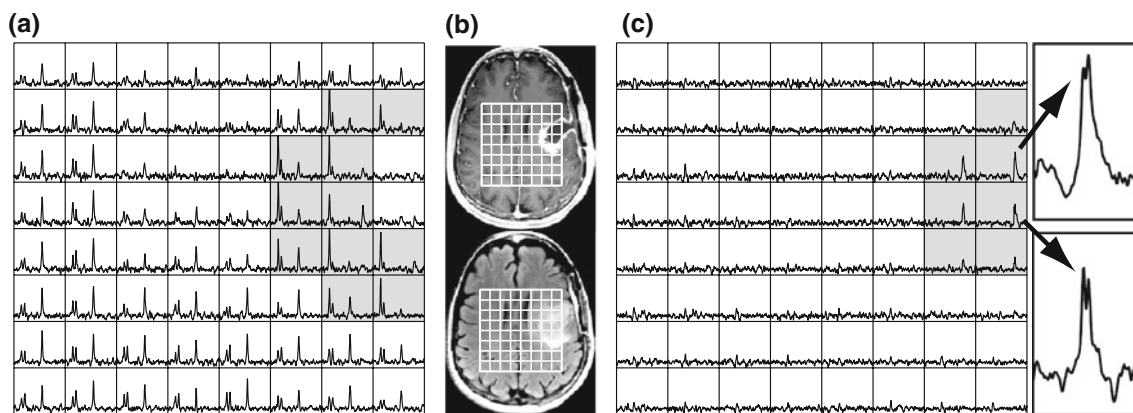


FIGURE 10. An example of lactate-edited spectra using the flyback-gradient method from a patient, showing the full coverage of a slice from the PRESS volume. In the summed spectra (a), the highlighted voxels show abnormal levels of metabolites with highly elevated choline around lesions in T1 post-contrast image (top, b) and T2-weighted FLAIR image (bottom, b). The highlighted voxels in the subtracted spectra (c) show lactate doublet at 1.3 ppm.

clearly visible as indicated in the zoomed-in spectra even with the presence of lipid. The voxel in the contralateral hemisphere contained normal levels of Cho, Cr, and NAA (c) with no lactate in the corresponding subtracted spectrum.

Another example of a patient exam that was acquired with the lactate-edited MRSI using a flyback echo-planar readout gradient is shown in Fig. 10. This shows the summed and subtracted spectra for the full coverage of a slice from the PRESS volume. The T2-weighted image from this patient (bottom in b) showed a large area of T2h in the left hemisphere, which consisted of a large necrotic area surrounded by a contrast enhancing rim, as depicted in T1-weighted post-contrast image (top in b). The summed spectra (a) showed abnormal levels of brain metabolites with high Cho and low NAA in the CEL and T2h. Several voxels in the necrotic area contained lipid. In the subtracted spectra (c), lactate doublet peaks were observed in the lesions.

DISCUSSION

This study demonstrated the feasibility of detecting lactate, as well as Cho, Cr, NAA, and lipid in 9.5 min using a new 3 T lactate-edited PRESS 3D MRSI sequence with a flyback echo-planar readout gradient. Using this approach, we were able to detect lactate in patients with brain tumors (median normalized SNR = 17) using a nominal voxel size of 1 cc and a factor of two reduction in scan time compared to conventional elliptical phase encoding MRSI (19 min).

Implementation of higher-bandwidth volume selection pulses was required because of the increased chemical shift between lactate methyl (1.3 ppm) and

methine (4.1 ppm) resonances at higher field. It should be noted that the bandwidth of slice selective 180° pulses in the current study (1500 Hz) was higher than those reported in the previous studies (ranging from 874 to 1385 Hz) which used a PRESS scheme for volume selection at 3 T.^{14,16,28} The use of higher-bandwidth pulses was important in minimizing chemical shift mis-registration because the chemical shift artifact is inversely proportional to the size of the RF bandwidth used for localization. The use of an over-PRESS factor and high bandwidth VSS pulses further minimized artifacts from chemical shift mis-registration.

Over-PRESS factors of 1.2, 1.5, and 1.7 were tested in this study in order to minimize the chemical shift mis-registration of two lactate resonances as well as other metabolites. Although the higher factor would have given more uniform lactate signal and metabolite ratios, an over-PRESS factor of 1.5 was used for all volunteer and patient scans because of the proximity of the excited volume to the subject's skull and the potential of having increased contamination from subcutaneous lipid with an 1.7 over-PRESS factor.

Although, in theory, the chemical shift artifact should be eliminated with an 1.5 over-PRESS factor since the excited box (91×102 mm) is bigger than the prescribed box (80×80 mm) (Fig. 3b), the lactate spectra with an 1.5 over-PRESS factor were still not completely uniform. Imperfections in slice selection may have contributed to the artifact. The lactate signal in the left column was relatively smaller than those in the rest of the excited volume, however, the variation of lactate level over the entire excited volume was relatively small and showed significant improvement over the lactate spectra acquired with the over-PRESS factor of 1.2 (Fig. 5). The lactate SNRs in regions

besides the left column were very uniform for the over-PRESS factor of 1.5 with the SD of 0.5 (Fig. 4). When interpreting lactate peaks in the left column, one should note the possibility of underestimating lactate in this region and may use other means to correct for the chemical shift artifacts. This can either be achieved using theoretical corrections that are determined from the size of the PRESS selected volume, the over-PRESS factor and the bandwidths of the selection pulses or to acquire empirical data with similar parameters from a uniform phantom and use the ratio of lactate intensities in different voxels to provide correction factors.

The trade-off in using a flyback echo-planar readout gradient is a decrease in sensitivity. The median signal reduction for the flyback echo-planar readout gradient compared to the conventional phase encoding in the normalized SNR of NAA was 17% for phantom and 22% for volunteers (Table 3), which are similar to previous findings described by Cunningham *et al.*³ The loss of data during rewind portion of the flyback trajectory and imperfections in the gradient trajectory contributed to the net signal loss. Lactate peaks with SNR smaller than 4 were difficult to be distinguished from noise, and therefore the SNR of 4 was used as a threshold for calculating the median SNR of lactate in patients. Although the conventional phase encoding method may provide higher sensitivity for lactate detection, especially when lactate concentration in tumors is small, the long scan time (20 min) has traditionally prevented it from being used in routine clinical practices. By integrating the flyback echo-planar readout gradient, we have made possible a factor of two reduction in scan time (9.5 min). As the use of 3 T scanner becomes more widespread due to its improved SNR associated with higher field strength, this technique is expected to be more appropriate for routine clinical uses and may assist in evaluating the role of lactate in the management of brain tumors.

In most cases, the highest lactate signal was observed in necrosis or resection cavity with a raw SNR as high as 18 in these regions. It is known that lactate produced in cancerous cells can accumulate in cystic or necrotic regions.¹³ Since lactate in these regions has been reported to be clinically irrelevant,² we limited our estimation of lactate signal to CEL or T2h and excluded lactate in necrosis and resection cavity.

The current study was primarily aimed at demonstrating the practicability of detecting lactate signal using the new lactate-edited 3D MRSI sequence in patients with brain tumors at 3 T; hence the clinical interpretation of lactate was omitted. A study assessing the patterns of lactate prior to radiation and during treatment in GBM patients is currently underway in an attempt to predict treatment outcome.

CONCLUSIONS

We have developed and implemented a lactate-edited 3D MRSI sequence that incorporates specialized rf pulses and a flyback echo-planar readout gradient at 3 T. The results from the current work demonstrated the ability of this sequence to detect lactate in the presence of lipid signal from brain tumor patients in a clinically acceptable acquisition time of 9.5 min. While further studies are required, this robust technique should permit non-invasive measurement of brain lactate as well as Cho, Cr, NAA, and lipid in routine clinical settings at 3 T and may assist in investigating its potential as a marker for prognosis and response to therapy.

ACKNOWLEDGMENTS

This study was partially supported by an academic-industry research grant ITL-BIO04-10148, which is funded by the UC Discovery Program in conjunction with GE Healthcare, and by NIH grants R01CA059880 and R01CA127612.

OPEN ACCESS

This article is distributed under the terms of the Creative Commons Attribution Noncommercial License which permits any noncommercial use, distribution, and reproduction in any medium, provided the original author(s) and source are credited.

REFERENCES

- ¹Aboagye, E. O., Z. M. Bhujwala, Q. He, and J. D. Glickson. Evaluation of lactate as a ¹H nuclear magnetic resonance spectroscopy index for noninvasive prediction and early detection of tumor response to radiation therapy in EMT6 tumors. *Radiat. Res.* 150:38–42, 1998.
- ²Crawford, F. W., I. S. Khayal, C. McGue, S. Saraswathy, A. Pirzkall, S. Cha, K. R. Lamborn, S. M. Chang, M. S. Berger, and S. J. Nelson. Relationship of pre-surgery metabolic and physiological MR imaging parameters to survival for patients with untreated GBM. *J. Neurooncol.* 91:337–351, 2009.
- ³Cunningham, C. H., D. B. Vigneron, A. P. Chen, D. Xu, S. J. Nelson, R. E. Hurd, D. A. Kelley, and J. M. Pauly. Design of flyback echo-planar readout gradients for magnetic resonance spectroscopic imaging. *Magn. Reson. Med.* 54:1286–1289, 2005.
- ⁴De Coene, B., J. V. Hajnal, P. Gatehouse, D. B. Longmore, S. J. White, A. Oatridge, J. M. Pennock, I. R. Young, and G. M. Bydder. MR of the brain using fluid-attenuated inversion recovery (FLAIR) pulse sequences. *AJNR Am. J. Neuroradiol.* 13:1555–1564, 1992.

- ⁵Di Costanzo, A., T. Scarabino, F. Trojsi, T. Popolizio, D. Catapano, G. M. Giannatempo, S. Bonavita, M. Portaluri, M. Tosetti, V. A. d'Angelo, U. Salvolini, and G. Tedeschi. Proton MR spectroscopy of cerebral gliomas at 3 T: spatial heterogeneity, and tumour grade and extent. *Eur. Radiol.* 18:1727–1735, 2008.
- ⁶Edden, R. A., M. Schar, A. E. Hillis, and P. B. Barker. Optimized detection of lactate at high fields using inner volume saturation. *Magn. Reson. Med.* 56:912–917, 2006.
- ⁷He, Q., Z. M. Bhujwalla, and J. D. Glickson. Proton detection of choline and lactate in EMT6 tumors by spin-echo-enhanced selective multiple-quantum-coherence transfer. *J. Magn. Reson. B* 112:18–25, 1996.
- ⁸Herholz, K., W. Heindel, P. R. Luyten, J. A. denHollander, U. Pietrzyk, J. Voges, H. Kugel, G. Friedmann, and W. D. Heiss. In vivo imaging of glucose consumption and lactate concentration in human gliomas. *Ann. Neurol.* 31:319–327, 1992.
- ⁹Kaiser, L. G., K. Young, and G. B. Matson. Elimination of spatial interference in PRESS-localized editing spectroscopy. *Magn. Reson. Med.* 58:813–818, 2007.
- ¹⁰Kelley, D. A., L. L. Wald, and J. M. Star-Lack. Lactate detection at 3T: compensating J coupling effects with BASING. *J. Magn. Reson. Imaging* 9:732–737, 1999.
- ¹¹Kim, S. H., K. H. Chang, I. C. Song, M. H. Han, H. C. Kim, H. S. Kang, and M. C. Han. Brain abscess and brain tumor: discrimination with in vivo H-1 MR spectroscopy. *Radiology* 204:239–245, 1997.
- ¹²Kim, J. H., K. H. Chang, D. G. Na, I. C. Song, B. J. Kwon, M. H. Han, and K. Kim. 3T ¹H-MR spectroscopy in grading of cerebral gliomas: comparison of short and intermediate echo time sequences. *AJNR Am. J. Neuroradiol.* 27:1412–1418, 2006.
- ¹³Kugel, H., W. Heindel, R. I. Ernestus, J. Bunke, R. du Mesnil, and G. Friedmann. Human brain tumors: spectral patterns detected with localized H-1 MR spectroscopy. *Radiology* 183:701–709, 1992.
- ¹⁴Lange, T., U. Dydak, T. P. Roberts, H. A. Rowley, M. Bjeljac, and P. Boesiger. Pitfalls in lactate measurements at 3T. *AJNR Am. J. Neuroradiol.* 27:895–901, 2006.
- ¹⁵Li, X., D. B. Vigneron, S. Cha, E. E. Graves, F. Crawford, S. M. Chang, and S. J. Nelson. Relationship of MR-derived lactate, mobile lipids, and relative blood volume for gliomas in vivo. *AJNR Am. J. Neuroradiol.* 26:760–769, 2005.
- ¹⁶Li, Y., J. A. Osorio, E. Ozturk-Isik, A. P. Chen, D. Xu, J. C. Crane, S. Cha, S. Chang, M. S. Berger, D. B. Vigneron, and S. J. Nelson. Considerations in applying 3D PRESS H-1 brain MRSI with an eight-channel phased-array coil at 3 T. *Magn. Reson. Imaging* 24:1295–1302, 2006.
- ¹⁷MacFall, J. R., N. J. Pelc, and R. M. Vavrek. Correction of spatially dependent phase shifts for partial Fourier imaging. *Magn. Reson. Imaging* 6:143–155, 1988.
- ¹⁸Margosian, P. Faster MR imaging: imaging with half the data. *Health Care Instrum.* 1:195–197, 1986.
- ¹⁹Nelson, S. J. Analysis of volume MRI and MR spectroscopic imaging data for the evaluation of patients with brain tumors. *Magn. Reson. Med.* 46:228–239, 2001.
- ²⁰Otazo, R., B. Mueller, K. Ugurbil, L. Wald, and S. Posse. Signal-to-noise ratio and spectral linewidth improvements between 1.5 and 7 Tesla in proton echo-planar spectroscopic imaging. *Magn. Reson. Med.* 56:1200–1210, 2006.
- ²¹Ozturk-Isik, E., J. C. Crane, S. Cha, S. M. Chang, M. S. Berger, and S. J. Nelson. Unaliasing lipid contamination for MR spectroscopic imaging of gliomas at 3T using sensitivity encoding (SENSE). *Magn. Reson. Med.* 55:1164–1169, 2006.
- ²²Ozturk-Isik, E., A. P. Chen, J. C. Crane, W. Bian, D. Xu, E. T. Han, S. M. Chang, D. B. Vigneron, and S. J. Nelson. 3D sensitivity encoded ellipsoidal MR spectroscopic imaging of gliomas at 3T. *Magn. Reson. Imaging* 27:1249–1257, 2009.
- ²³Pauly, J., P. Le Roux, D. Nishimura, and A. Macovski. Parameter relations for the Shinnar-Le Roux selective excitation pulse design algorithm [NMR imaging]. *IEEE Trans. Med. Imaging* 10:53–65, 1991.
- ²⁴Prichard, J. W. What the clinician can learn from MRS lactate measurements. *NMR Biomed.* 4:99–102, 1991.
- ²⁵Pruessmann, K. P., M. Weiger, M. B. Scheidegger, and P. Boesiger. SENSE: sensitivity encoding for fast MRI. *Magn. Reson. Med.* 42:952–962, 1999.
- ²⁶Saraswathy, S., F. W. Crawford, K. R. Lamborn, A. Pirzkall, S. Chang, S. Cha, and S. J. Nelson. Evaluation of MR markers that predict survival in patients with newly diagnosed GBM prior to adjuvant therapy. *J. Neurooncol.* 91:69–81, 2009.
- ²⁷Sijens, P. E., P. C. Levendag, C. J. Vecht, P. van Dijk, and M. Oudkerk. ¹H MR spectroscopy detection of lipids and lactate in metastatic brain tumors. *NMR Biomed.* 9:65–71, 1996.
- ²⁸Smith, M. A., J. A. Koutcher, and K. L. Zakian. J-difference lactate editing at 3.0 Tesla in the presence of strong lipids. *J. Magn. Reson. Imaging* 28:1492–1498, 2008.
- ²⁹Star-Lack, J., D. Spielman, E. Adalsteinsson, J. Kurhanewicz, D. J. Terris, and D. B. Vigneron. In vivo lactate editing with simultaneous detection of choline, creatine, NAA, and lipid singlets at 1.5 T using PRESS excitation with applications to the study of brain and head and neck tumors. *J. Magn. Reson.* 133:243–254, 1998.
- ³⁰Tran, T. K., D. B. Vigneron, N. Sailasuta, J. Tropp, P. Le Roux, J. Kurhanewicz, S. Nelson, and R. Hurd. Very selective suppression pulses for clinical MRSI studies of brain and prostate cancer. *Magn. Reson. Med.* 43:23–33, 2000.
- ³¹Warburg, O. On the origin of cancer cells. *Science* 123:309–314, 1956.
- ³²Weybright, P., P. C. Sundgren, P. Maly, D. G. Hassan, B. Nan, S. Rohrer, and L. Junck. Differentiation between brain tumor recurrence and radiation injury using MR spectroscopy. *AJR Am. J. Roentgenol.* 185:1471–1476, 2005.
- ³³Zierhut, M. L., E. Ozturk-Isik, A. P. Chen, I. Park, D. B. Vigneron, and S. J. Nelson. (1)H spectroscopic imaging of human brain at 3 Tesla: comparison of fast three-dimensional magnetic resonance spectroscopic imaging techniques. *J. Magn. Reson. Imaging* 30:473–480, 2009.